Icarus 201 (2009) 217–225

Contents lists available at ScienceDirect

Icarus

www.elsevier.com/locate/icarus

Shoreline features of Titan's Ontario Lacus from *Cassini*/VIMS observations

Jason W. Barnes [a,b,*], Robert H. Brown [c], Jason M. Soderblom [c], Laurence A. Soderblom [d], Ralf Jaumann [e], Brian Jackson [c], Stéphane Le Mouélic [f], Christophe Sotin [g], Bonnie J. Buratti [g], Karly M. Pitman [g], Kevin H. Baines [g], Roger N. Clark [h], Phillip D. Nicholson [i], Elizabeth P. Turtle [j], Jason Perry [c]

[a] *NASA Ames Research Center, Mail Stop 244-30, Moffett Field, CA 94035, USA*
[b] *Department of Physics, University of Idaho, Engineering-Physics Building, Moscow, ID 83844, USA*
[c] *Department of Planetary Sciences, University of Arizona, Tucson, AZ 85721, USA*
[d] *United States Geological Survey, Flagstaff, AZ 86001, USA*
[e] *DLR, Institute of Planetary Research, Rutherfordstrasse 2, D-12489, Berlin, Germany*
[f] *Laboratoire de Planétologie et Géodynamique, CNRS UMR6112, Université de Nantes, France*
[g] *Jet Propulsion Laboratory, California Institute of Technology, 4800 Oak Grove Drive, Pasadena, CA 91109, USA*
[h] *United States Geological Survey, Denver, CO 80225, USA*
[i] *Department of Astronomy, Cornell University, Ithaca, NY 14853, USA*
[j] *Johns Hopkins University Applied Physics Laboratory, 11100 Johns Hopkins Road, Laurel, MD 20723, USA*

ARTICLE INFO

Article history:
Received 23 July 2008
Revised 3 December 2008
Accepted 15 December 2008
Available online 6 January 2009

Keywords:
Titan

ABSTRACT

We analyze observations of Titan's south polar lake Ontario Lacus obtained by *Cassini*'s Visual and Infrared Mapping Spectrometer during the 38th flyby of Titan (T38; 2007 December 5). These near-closest-approach observations have the highest signal-to-noise, the finest spatial resolution, and the least atmospheric influence of any near-infrared lake observation to date. We use the large, spatially flat, and low-albedo interior of Ontario Lacus as a calibration target allowing us to derive an analytical atmospheric correction for emission angle. The dark lake interior is surrounded by two separate annuli that follow the lake interior's contours. The inner annulus is uniformly dark, but not so much as the interior lake, and is generally 5–10 kilometers wide at the lake's southeastern margin. We propose that it represents wet lakebed sediments exposed by either tidal sloshing of the lake or seasonal methane loss leading to lower lake-volume. The exterior annulus is bright and shows a spectrum consistent with a relatively low water-ice content relative to the rest of Titan. It may represent fine-grained condensate deposits from a past era of higher lake level. Together, the annuli seem to indicate that the lake level for Ontario Lacus has changed over time. This hypothesis can be tested with observations scheduled for future Titan flybys.

1. Introduction

The discovery of probable lakes near Titan's north pole in *Cassini* observations (Stofan et al., 2007) represents the culmination of many years spent in anticipation of finding surface liquids on Titan (*e.g.* Sagan and Dermott, 1982; Lunine et al., 1983; Lunine, 1993). Though there is no global ocean (West et al., 2005), the estimated fractional coverage of Titan's surface area by liquid, ~1% (Hayes et al., 2008), matches the theoretical prediction made by Mitri et al. (2007) based on global humidity. The recent *Cassini* Visual and Infrared Mapping Spectrometer (VIMS; Brown et al., 2004) detection of absorption features attributed to liquid ethane within putative lakes (Brown et al., 2008) provides the "smoking gun" confirming their lacustrine nature.

The geographic distribution of the lakes, clustered within ~20 degrees of the poles (Stofan et al., 2007; Turtle et al., 2009), seems to derive from a combination of atmospheric global circulation and the net transport of volatiles into the coldest regions. Titan's tropics are a vast desert, as evidenced by the long-term presence of sand dunes there (Lorenz et al., 2006; Radebaugh et al., 2008; Barnes et al., 2008). Global circulation models by Rannou et al. (2006) show that clouds, and presumably rain, prevail both at the poles and at 40° latitude in the summer hemisphere. They are rare elsewhere. Observations both from the ground (Roe et al., 2002, 2005; Brown et al., 2002) and from *Cassini* (Porco et al., 2005; Rodriguez et al., 2009) first indicated this nonuniform cloud distribution.

So if it rains both at the poles and at 40° N and 40° S, why are there lakes at only the poles? The lakes' composition may provide

* Corresponding author at: NASA Ames Research Center, Mail Stop 244-30, Moffett Field, CA 94035, USA.
E-mail address: jason@barnesos.net (J.W. Barnes).

0019-1035/$ – see front matter
doi:10.1016/j.icarus.2008.12.028

a clue. If the lakes have a significant ethane component, as spectral analysis indicates (Brown et al., 2008), then where methane rains down may not spatially correlate with the locations of ethane rain. Griffith et al. (2006) show that clouds seen over the dark, winter pole with downwelling air currents are probably composed of ethane rather than methane. Hence temperate methane rainfall may be rather ephemeral on the surface, evaporating away quickly back into the atmosphere, while ethane rainfall at the poles is less easily redistributed owing to ethane's much lower vapor pressure at Titan's surface temperatures. It is also possible that the atmospheric conditions in the mid-latitude preclude rainfall from reaching Titan's surface.

The lakes as seen from *Cassini* come in a variety of shapes and sizes. The RADAR instrument in its synthetic aperture radar (SAR) mode has observed lakes near the north pole that are variously small (a few kilometers across) and circular; moderately sized (tens to hundreds of km across), some with smooth, regularly scalloped edges and others resembling terrestrial reservoirs; and vast seas thousands of km across (Stofan et al., 2007; Hayes et al., 2008; Mitchell, in preparation). Some RADAR "lakes" may presently be dry, possibly having been drained by evaporation or subsurface hydraulic flow (Hayes et al., 2008). The Imaging Science Subsystem (ISS), which images Titan's surface at a near-infrared wavelength of 0.938 μm, also observed very-low-albedo, regularly shaped features near the south pole that the team interpreted to be lakes (Turtle et al., 2009).

High-resolution intercomparison of VIMS/ISS near-infrared imaging and RADAR observations of the same lacustrine features has not been possible to this point. The spacecraft's trajectory along with an on-board computer glitch on the T7 flyby (2005 September 7) have conspired to produce RADAR views of only the north pole prior to T39 (2007 December 20). Near-infrared imaging, reliant on solar illumination, is presently best able to view the southern, summer pole. However, Brown et al. (2008) showed that RADAR and VIMS were both able to see the same large, dark northern sea using atmospheric scattering to indirectly illuminate onto the night side of Titan's terminator. ISS also has this capability (Turtle et al., 2009).

On the recent T38 (2007 December 5) *Cassini* flyby of Titan, VIMS observed the south polar lake Ontario Lacus during closest approach. Brown et al. (2008) used these observations to spectroscopically identify ethane in this lake. In this paper, we use the VIMS T38 observations, along with ISS rev9 (2005 June 6) imaging for context, to investigate the geomorphology and shoreline features associated with Ontario Lacus. We first describe the observations themselves and the data reduction process that we used to prepare the data for analysis. Next we analyze the observations, and we suggest and investigate various hypotheses for the characteristics that we see. Finally we discuss the implications of our findings, compare our observations to radar observations of different lakes, and make predictions for future RADAR topographic and SAR observations of Ontario Lacus in the Cassini Equinox Mission.

2. Observations

2.1. Data acquisition

The T38 flyby was designed to optimize spectroscopy. The VIMS spectral mapping cubes acquired thus have long integration times to improve the signal-to-noise ratio. Although they were not the primary deliverable of the VIMS T38 flyby design, the T38 images acquired by VIMS complement the high S/N spectroscopy and provide the opportunity for serendipitous additional science. The flyby design targeted the edge of Ontario Lacus in order to allow comparison of the lake spectra to those of adjacent regions to calibrate atmospheric effects. However, spatial coverage of Ontario Lacus was incomplete due to the geometry of the encounter and the very limited time near closest approach.

Table 1
VIMS T38 Ontario Lacus observations.

Cube title	Cube dims (pixels)	Emission angle (S/C)	Exp times (ms)	Mode	Best spatial resolution (m)
CM_157550**6608**_1	48 × 48	22°–41°	80	Noodle	330
CM_157550**6843**_1	64 × 32	47°–70°	180	Cube	830
CM_157550**7241**_1	64 × 32	70°–79°	180	Cube	1540
CM_157550**7643**_1	64 × 32	78°–90°(+)	180	Cube	2500

A total of four cubes were acquired (see Table 1 and Fig. 1). The spacecraft trajectory took *Cassini* directly over Ontario Lacus, which is centered near 74° S, 180° W. The spacecraft moves so rapidly relative to Titan near closest approach that it is unable to track targets on the surface. The first cube (which we will refer to by the last four digits of its file designation: 6608) was acquired just after closest approach (1300 km from the surface for T38), so it uses the "noodle" mode that was developed for the T20 (2006 October 25) flyby and is described in Barnes et al. (2008). As *Cassini* flew away from Titan, it was then able to track surface targets and the other three cubes (6843, 7241, and 7639) were acquired in imaging mode.

For the bulk of the data reduction we proceed following the standard VIMS processing pipeline for imaging (Barnes et al., 2007a) and noodle (Barnes et al., 2008) cubes: background subtraction, cosmic ray cleaning, flatfield correction, flux calibration, and geometric mapping. However, cubes 6843 and 7241 show a scattered-light component that varies substantially over the course of the cubes' acquisition time. This component presumably results from light that is not blocked by VIMS' shutter because it shows up in the instrument's on-board background measurements and displays marked variability across the IR detector's filter gaps. Its magnitude is comparable to that of the instrumental background signal.

To remove the scattered-light component we use the original, on-board background measurements as a record of their intensity. First we coadd all of the background measurements from each cube to establish the spectral character of the scattered light. We then fit the background measurement for each line by with a linear fit to the above average in order to improve the background signal-to-noise ratio and to eliminate cosmic ray hits. We then subtract the resulting inferred total background measurement, temporally interpolated between each background measurement for every individual pixel as the background varies significantly between individual lines of the cube.

The scattered-light component appears only in a total of four VIMS Titan cubes from the entire mission so far: those from Tortola Facula on Ta (2004 October 26), PacMan Bay on T20 (Jaumann et al., 2008), and then 6843 and 7241 from T38 as described here. Among the VIMS Titan dataset, these cubes are the ones obtained while closest proximity to Titan's surface (within ~3000 km; Barnes et al., 2009). While we expect, then, that future observations acquired at low altitudes will also show a significant scattered-light component, we have shown here that it can be identified and removed and thus will not affect science results.

The four T38 cubes observe roughly the same area but at different spatial resolutions, integration times, and emission angles (Table 1). Because spacecraft orientation restrictions prevented nadir observations near closest approach, even the noodle cube has a nonzero emission angle. As a result, a method for compensating for the atmosphere's effects is necessary in order to be able to compare between the cubes. While atmospheric removal is the ultimate goal of near-infrared data processing of Titan data, a method to do so that accounts for spatially and temporally nonuniform

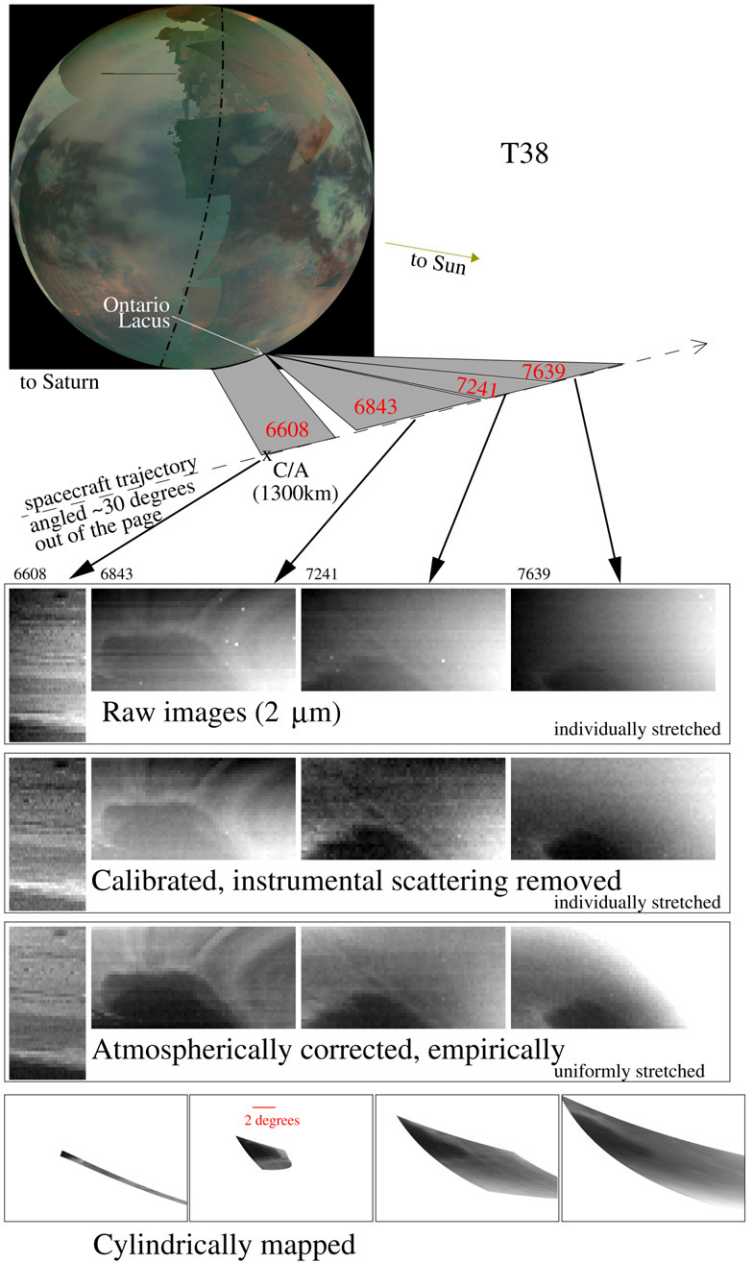

Fig. 1. This diagram shows the observational geometry of the VIMS T38 Ontario Lacus observations. The diagram is approximately to scale, but is not meant to be a precise navigational chart. Titan and the spacecraft trajectory are shown from a perspective a fixed distance above Titan's equator at 90° E longitude, with Saturn to the left and the Sun off-page to the right (and slightly into the page). The dot-dashed line on Titan represents the terminator; night is on the left-hand side. Ontario Lacus, 74° S, 180° W, is on the moon's limb (white arrow). The four VIMS observations (see Table 1) are shown, along with various stages of data reduction as described in the text.

haze, phase effects, and Titan's atmospheric geometry is still being developed. Though we do not present a fully robust solution here, the T38 observations themselves allow us to determine a partial, *empirical* correction. To do so we use Ontario Lacus as a calibration target.

2.2. Data reduction

Because it is a spatially extended, well-resolved, uniform spectral unit, and because the T38 observations provide four separate views of the same area with different emission angles but nearly identical incidence angles, we are able to disentangle the competing effects of incidence and emission angle when characterizing radiative transfer in Titan's atmosphere. We show the measured I/F values within the inner portion of Ontario Lacus as the black points in Fig. 2. The I/F values measured as a function of emission angle for a nearby brighter and also relatively uniform area on the surface are shown as red points.

To characterize both the additive component of I/F due to atmospheric scattering and the component due to atmospheric attenuation, we fit the data using a simple, analytic single-scattering approximation. While this model is only technically accurate when the atmospheric optical depth is low, we find that, with appropriate adjustments, it can fit higher optical depth cases as well. We fit for I/F heading upward out of Titan's atmosphere, and as measured by VIMS, as a function of the incidence (P_I) and emission (P_E) path lengths in units of normally incident atmospheres (*i.e.*, one trip straight through the atmosphere at nadir, that has an optical depth equal to τ, would equal 1.0 atmospheres — thus what we are calling "path length" is what ground-based astronomers call the airmass).

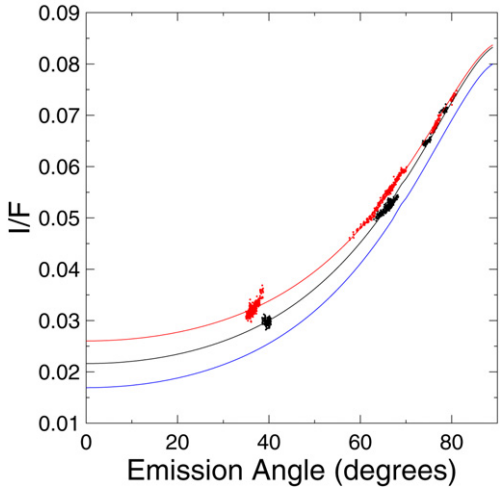

Fig. 2. VIMS-measured emission phase function for the Ontario Lacus interior (black points) and a uniform, brighter area outside the lake (red points) at 2.018 μm. The lines represent Eq. (1) as fit for this channel. The best-fit values for this channel were $\tau = 0.147$, $\varpi = 1.12$, and $f = 4.36$. The bottom, blue curve illustrates the values for $A = 0$, the black curve for $A = 0.036$, and the red curve for $A = 0.083$. The best-fit lines were generated using average incidence angle values for the scene. The leftmost cluster of red points diverges from the fit because those points were obtained in the noodle cube (6608), and so have phase angle changing with time, while the other cubes fortuitously have stable phase angles. We plotted the red curve assuming a single phase value.

$$\frac{I+}{F} = Ae^{-\tau(fP_I+P_E)} + \varpi\frac{(fP_I)^{-1}}{(fP_I)^{-1}+P_E^{-1}}\left(1-e^{-\tau(fP_I+P_E)}\right) \qquad (1)$$

with A as the surface albedo, $I+$ as the light intensity heading outward at the top of the atmosphere, and ϖ as the effective albedo of the atmosphere (and incorporates atmospheric absorption). The adjustment to a conventional single-scattering model is the parameter f that modifies P_I is a fudge-factor to account for forward-scattering of light, decoupling P_I from P_E.

To calculate P_I and P_E from the incidence and emission angles respectively, we represent Titan's atmosphere as a uniform, spherical shell 150 km high sitting on top of the surface. We then numerically determine the path length P as a function of zenith angle, interpolating through a table for computational efficiency. We tried other vertical atmospheric profiles including exponential, blocks of differing heights, and the actual density profile as measured by the *Huygens* probe (Fulchignoni et al., 2005), but the 150 km orange-rind fit the data best of any models that we tried. Given that our goal is strictly an empirical fit for surface intercomparison, and not to model the atmosphere in and of itself, we use this atmospheric representation that results in the best fits to the emission phase function.

We use a Leavenberg–Marquardt χ^2 minimization fitting algorithm to fit for τ, ϖ, and f. For areas with high signal-to-noise, we fit for the both albedo A of the lake interior and that of the brighter area; where the signal-to-noise is low, in the 2.7 μm, 2.8 μm, and 5.0 μm windows, we fix the albedo of the lake interior at zero. An example emission phase function fit is shown in Fig. 2 for the 2.01 μm channel.

At 2 μm and shorter, the lake interior is best fit with a nonzero albedo, though the actual albedo value used is not meaningful. The larger value stems from the fit attempting to account for multiple-scattering terms. The values that we are calling "albedo" here vary monotonically with the actual surface albedo, but the values themselves are not representative of the actual surface reflectance. Hence the absolute values cannot be used scientifically. The correction does, however, allow for a relative comparison of surface reflectance between VIMS cubes taken of the same area with varying emission angle.

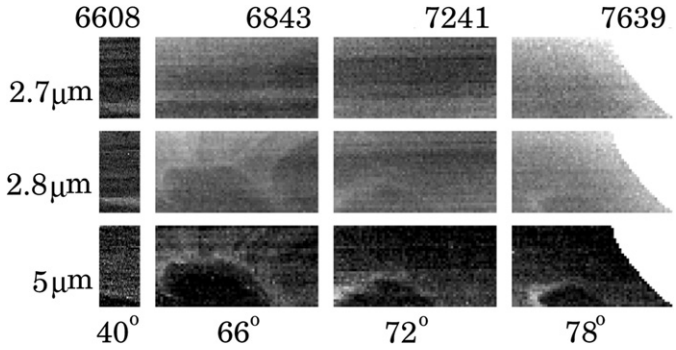

Fig. 3. The four VIMS T38 cubes of Ontario Lacus at 2.7 μm (top), 2.8 μm (middle), and 5 μm (bottom). Using the 5 μm image for reference, the shoreline of Ontario Lacus is visible near the bottom-left of each image. The shoreline is visible in each cube at 2.8 μm, but becomes increasingly difficult to discern at 2.7 μm as the emission angle (noted at bottom) increases. The lake is not visible in the highest emission angle cube, 7639. The different behavior of the emission phase function at 2.7 μm relative to that at 2.8 μm implies that Titan's atmosphere absorbs more strongly at 2.7 μm than it does at 2.8 μm. This effect must be compensated for when interpreting surface spectra in terms of composition.

2.3. Atmospheric implications

The four observations at differing emission angles can also be used to constrain the nature of the absorption spectrum of Titan's atmosphere. In particular the atmospheric absorption component that influences Titan's 2.7 μm and 2.8 μm spectral windows remains poorly understood. As a result the interpretation of surface spectra in this region is ambiguous. McCord et al. (2008) attribute a positive 2.7 μm to 2.8 μm slope within Titan's 5-μm bright areas as evidence that those regions contain carbon dioxide frost, whose spectrum also shows a positive 2.7/2.8 μm slope. Clark et al. (in preparation) suggest that Titan's nearly-global positive 2.7/2.8 μm slope rules out the presence of significant quantities of surficial water ice, which has a steep negative slope between 2.7 μm and 2.8 μm. Both of these interpretations assume that the relative atmospheric transmission between the 2.7 μm and 2.8 μm windows is uniform, and hence that the positive 2.7/2.8 μm slope derives from surface reflectance.

If Titan's atmosphere absorbs more light at 2.7 μm than at 2.8 μm, however, then a different interpretation emerges. In this scenario the high 2.8/2.7 μm ratio of the 5-μm bright regions could still be the result of a surface component that also shows a high 2.8/2.7 μm ratio, as suggested by McCord et al. (2008). But now that ratio might instead come about due to a relative *lack* of a component with a very low 2.8/2.7 μm ratio: water ice. This scenario has not been favored in the past because the 2.8/2.7 μm ratio all over Titan is near unity (Clark et al., in preparation), which would then require a particular combination of high surface reflectivity and low atmospheric transmission at 2.7 μm in order to lead to the same I/F as we see at 2.8 μm.

The VIMS T38 data address this question directly, if not quantitatively (see Fig. 3). The relative contrast of the lake interior and its surroundings is visible in all four cubes at 2.8 μm. Within the 2.7 μm band the lake contrast is visible in the lowest-emission-angle cube, 6608, and not at all in the cubes obtained at higher emission angle. Without two or more points on the emission phase function curve we cannot therefore derive quantitative measurements of the 2.7 μm atmospheric absorption. However, this qualitative behavior indicates that atmospheric absorption plays a significantly stronger role at 2.7 μm than it does at 2.8 μm. Hence we interpret the high 2.8/2.7 μm ratio of the 5-μm bright areas to in-

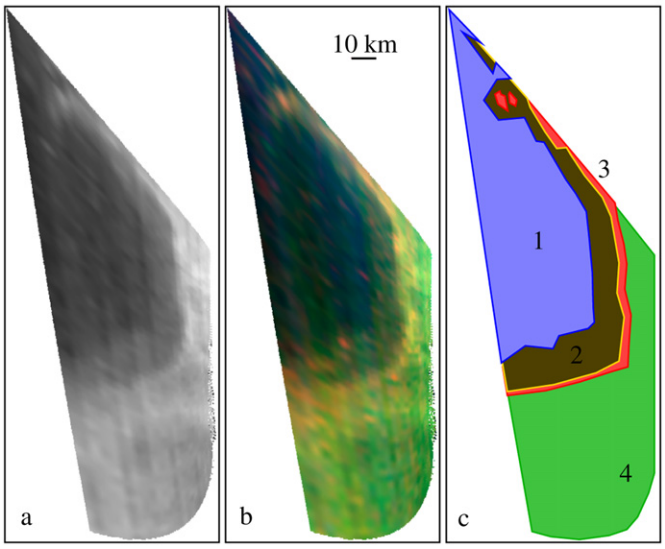

Fig. 4. VIMS cube CM_1575506843_1, shown in an orthographic projection from directly above the lake (74° S, 180° W). Subfigure (a) is a 2-μm image; (b) is a 3-color image with red as 5 μm, green as 2 μm, and blue as 1.6 μm; and (c) is a unit map, with units numbered. Unit 1 (blue) corresponds to the uniformly dark interior of Ontario Lacus. Unit 2 (yellow/brown) is a less-dark, uniform shelf that surrounds Unit 1. Unit 3 (red) is a narrow, bright annulus that exists at the edge of the lake. Unit 4 (green) represents the area exterior to the lake (the Unit 3/4 border is defined by inspection, and is somewhat arbitrary).

dicate a composition that is possibly very low in water ice relative to the rest of Titan.

3. Analysis

We show an orthographically projected view of the fine-spatial-resolution, long-integration-time (180 ms) cube 6843 in Fig. 4. This VIMS cube covers the southeastern margin of Ontario Lacus. It shows a complex system of spectral units at the lake's shoreline. The lake's interior, Unit 1, is very dark in each of the 6 most transparent of Titan's spectral windows (1.28 μm, 1.58 μm, 2.0 μm, 2.7 μm, 2.8 μm, and 5 μm). This unit is spatially uniform across its extent, consistent with the interpretation that it is a body of liquid hydrocarbon as shown by Brown et al. (2008).

The existence of two other spectral units, Units 2 and 3, surrounding the lake interior was not anticipated. Unit 2 is a well-resolved, spatially uniform strip immediately adjacent to the lake interior. The width of the strip varies gradually between 3 and 10 km. This unit is also dark at all wavelengths, but not as dark as Unit 1.

Unit 3 is a bright unit at 2 μm and is yet brighter at 5 μm relative to the lake exterior (Unit 4). For the most part, Unit 3 borders the exterior of Unit 2. One or a few small "islands" of Unit 3 jut into the lake near the north edge of cube 6843. This unit is not spatially resolved in cube 6843, and hence we can only place an upper limit of 2 km for its width using imaging alone.

We show an orthoprojected color mosaic of the four VIMS T38 cubes, along with ISS rev9 imaging (Turtle et al., 2009) for context, in Fig. 6. This view shows that Unit 3 continues around the eastern and northeastern margins of the lake. Based on the region where the VIMS and ISS views overlap, the bright margin on the west and southwest margins of the lake in the ISS view is likely an extension of Unit 3 as well. Unit 3 is much wider on both the eastern and southwestern sides than it is at the southeast — up to at least 10 km wide in some places.

Unit 2 is not visible farther north up the eastern coast of Ontario Lacus. This effect may be real, as the width of Unit 2 decreases to the north in cube 6843 (Fig. 4) as well. It may also be an artifact of lower spatial resolution and increased atmospheric scattering in cubes 7241 and 7643 relative to cube 6843. The ISS view may show indications of Unit 2 farther north, but given the uncertainties in atmospheric scattering effects on 0.938 μm Titan imaging and contrast the identification is tenuous.

4. Discussion

The concentric nature of the annuli surrounding the dark, central, liquid portion of Ontario Lacus implies that the rings and the lake are causally associated. Presumably the lake created Units 2 and 3 via lake level changes, shoreline processes, or some other phenomenon. Here we investigate several hypotheses regarding the formation of Unit 2 (the "shelf") and Unit 3 (the "bathtub ring").

4.1. Unit 2

4.1.1. Freeze/thaw

Though Titan's polar temperatures are thought to drop to near the freezing point of both methane (91 K) and ethane (90.3 K), dissolved atmospheric nitrogen ought to depress the freezing point of lake-borne liquids well below these values. In the event that freezing is possible on Titan, we examine whether the morphology that we see might result from freezing and/or thawing. On Earth lakes freeze from the top down, and thaw from the bottom up, because H_2O solid is less dense than H_2O liquid, and thus floats on top of it. On Titan the lakes ought to freeze from the bottom up, and to thaw from the top down, as solid hydrocarbons are more dense than their liquids and should settle to the bottom of a lake. A previously frozen lake in the process of thawing might then be expected to transition relatively quickly from one with a solid surface to one with a liquid surface. At no time would a thawing lake, then, develop a ring around its margin. A lake in the process of freezing might very well show a ring. As heat loss from the lake surface initiates freezing, the solids would fall to the lake bottom. As the freezing rate depends on surface area, then, and not on depth, the freezing might be expected to proceed at the same rate (in units of grams per square meter per day, perhaps) at the lake edges as at its center. Shallower areas would see their volumes fill with solid before deeper areas nearer the lake center. While the resulting solid-edged, creamy-center lake might resemble what VIMS sees in Fig. 4, where the albedo rules out a solid center of the lake (Brown et al., 2008), that cube was obtained near the end of Titan's 7-Earth-year south polar summer. Hence freezing is unlikely at the time of T38, and we reject the hypothesis that the lake is in the midst of a freezing or thawing cycle.

4.1.2. Continental shelf

In a body of liquid hydrocarbon that is sufficiently shallow, some light could penetrate to the lake bottom, where it would be reflected. Thus a bathymetric profile for the lake similar to that of Earth's oceans, with a bimodal depth regime shallow near the shoreline and deep far from the shore, can be constructed to reproduce Units 1 and 2. However, we reject this hypothesis for the nature of Unit 2 for several reasons. Because Unit 2 is spatially uniform in brightness, and because it has a sharp inner boundary with Unit 1, the inferred subaqueous topographic profile would be a stairstep — down at the outer edge of Unit 2, then of nearly uniform depth until the inner edge of Unit 2 where there would be a cliff-edge down to a liquid depth corresponding to very high optical depth. This bathymetric profile seems unlikely, though it could be produced by an unusual formation mechanism, perhaps with nested calderae (a possible formation mechanism suggested by, *e.g.*, Stofan et al., 2007). Though it is not altogether unlike that of Earth's continental shelves, there is no reason to think that a similar mechanism should lead to a bimodal depth regime inside

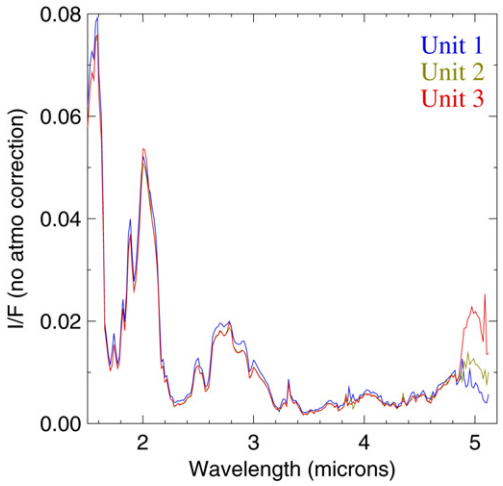

Fig. 5. VIMS spectra of the three spectral units from Ontario Lacus as outlined in Fig. 4. The spectra are not atmospherically corrected, and hence are dominated by atmospheric scattering and absorptions. The empirical correction discussed in the text does not result in meaningful absolute albedos that can be compared between VIMS wavelength channels. Unit 3 has a decidedly higher 5-micron I/F than Units 1 and 2; we attribute this difference to a relative dearth of water-ice (see text).

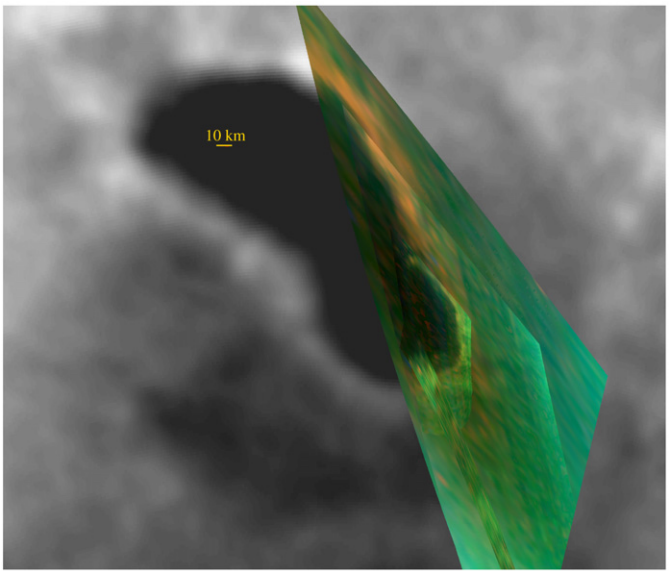

Fig. 6. Regional mosaic of the four T38 VIMS cubes (described in Table 1) with ISS rev9 image for context. The image is an orthographic projection from directly above the lake (74° S, 180° W). Relative geometry between the VIMS and ISS views was adjusted by hand; without updated SPICE kernels with Titan's new pole position (Stiles et al., 2008), the pipeline-generated automatic geometry has artificial offsets of up to 40 km.

Titan's lakes. Calculations of the mean free path for 2-μm photons in liquid methane show that reflections off the lake bottom could only detected for very shallow depths: no greater than a few tens of centimeters (Clark et al., in preparation).

4.1.3. Floating or suspended material

Unit 2 could result from scattering off of particles either floating on or suspended in liquid. In order to float, solid hydrocarbon material would need to be porous; in order to be both suspended and detected by VIMS, it would need to have a small particle size $>\sim$1 μm. Both formation of a foam and the suspension of particles would require turbulent mixing of the lake's liquid, as could perhaps occur from tidal sloshing (back-and-forth motion at the tidal frequency). In contrast, Brown et al. (2008) found that the lake interior (Unit 1) must be smooth and quiescent in order to explain the low 5-μm albedo (see Fig. 5). The spatial uniformity and sharp inner boundary of Unit 2 are thus not easy to explain via this mechanism, but given present data we cannot rule it out entirely. *Cassini* RADAR altimetry over the area, presently planned for T49 (2008 December 21), could support or refute this hypothesis: if the entirety of Unit 2 is the same altitude as the lake center, then foam or suspension could be likely candidates. If, on the other hand, Unit 2 shows a nonzero slope or a different elevation than Unit 1, floating or suspended particles would be ruled out.

4.1.4. Beach

Another idea for the nature of Unit 2 is that it might be a beach. Beaches on Earth are created and maintained by wave action against a shoreline. Hence in order to form a beach around Ontario Lacus, the lake itself would have to show wave activity of sufficient energy. By analogy, Earth's Lake Ontario, of similar size to Ontario Lacus, does show beaches in some areas. Lorenz et al. (2005) demonstrated that waves generated in liquid hydrocarbon (kerosene) are larger than those in water at equivalent air density and wind velocity. Hence if the winds near Titan's south pole become sufficiently strong for at least part of the year, then generation of beach-forming waves may not be unreasonable. There is, however, a problem of scale. The widest beaches on Earth are a few hundred meters wide. Unit 2 is 10 km in extent. RADAR has seen slightly brighter areas interpreted to be of shallower liquid on one side of some north polar lakes; these may represent the same process as Ontario Lacus' Unit 2 (Hayes et al., 2008). There are ocean shorelines on Earth that are many kilometers in width, however they form tidal mudflats, and not beaches.

4.1.5. Exposed lake-bottom sediments

The 'shelf' could correspond to areas where VIMS is seeing part of the lakebed that has been exposed as a result of either changes in the bulk volume of liquid within the lake or to tidal forcing. Titan shows pronounced changes in the distribution of clouds over its seasonal cycle (*e.g.* Rodriguez et al., 2009), and presumably has differences in precipitation as well. Seasonal transport of volatiles from the summer to the winter pole could then lead to seasonal changes in the level of Ontario Lacus. Unfortunately the VIMS coverage from T38 has sufficient signal-to-noise to detect Unit 2 only in cubes 6608 and 6843, which show just the south shore. The surrounding ISS view does show a moderate-albedo rim between the dark interior and the very bright surrounding material that may represent Unit 2 extending all of the way around the lake. VIMS will observe Ontario Lacus again, albeit at coarser spatial resolution, on T51 (2009 March 27).

The noodle cube 6608 shows a small dark spot that might represent a dry lakebed a few hundred km south of Ontario Lacus. If this spot is a lakebed, then it is evidently dry at present, as its albedo matches that of Unit 2 and not of Unit 1 (the portion of Ontario Lacus that is liquid; Brown et al., 2008). This second dry lakebed implies that the process drying up Ontario Lacus, if indeed that is what occurred, was widespread and not merely local. This assessment agrees with the interpretations from RADAR of a mixture of filled and dry lakes at the north pole (Hayes et al., 2008). Unfortunately VIMS has not yet acquired fine spatial resolution, low emission and inclination angle observations of the north polar RADAR lakes/lakebeds for purposes of direct intercomparison.

Intertidal zones are geographic areas that are both inundated at high tide and exposed at low tide. On Earth intertidal zones with shallow gradients are commonly covered with sediments as intertidal mudflats. The dark unit ringing the lake could represent sediments that have been exposed at low tide. Lorenz (1994) showed that on Titan, like on Earth, the effect of tides on isolated bodies of liquid changes the orientation of the effective gravity vector as

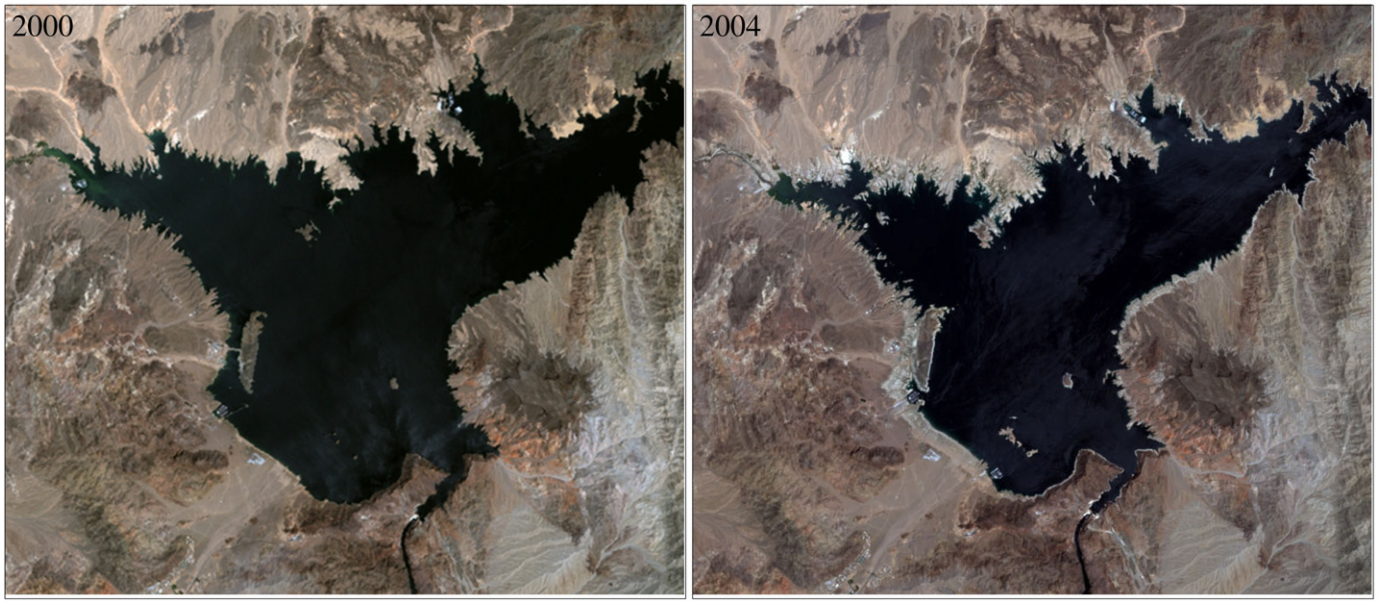

Fig. 7. Landsat 7 image of Lake Mead in Arizona, USA taken in 2000 (left) and again in 2004 after a prolonged drought (right). The drought has left a bright annulus around the lake that is thinner where the slope is high, and wider where the slope is low.

a function of orbital phase, leading to sloshing back-and-forth of lake-borne liquids. The total change in the slope s of an equipotential surface between periapsis and apoapsis for a point located along 0 or 180 degrees longitude is equal to $\frac{A}{R}\sin(2l)$ where l is the latitude of the point in question, R is the planet's radius, and A is the total tidal amplitude of an entirely fluid planet. Assuming that the planet's solid surface is rigid and does not deform under the tidal stresses, then the variation in the height of the north and south edges of a lake that is much smaller than the planet radius would be $A_{\text{lake}} = \frac{AL}{R}\sin(2l)$ where L is the total length of the lake in the north–south direction. Note, then, that lakes located at the equator and at the poles should show no tidal variation, while those at the mid-latitudes will show the greatest tidal amplitude. For Ontario Lacus, at 74° S and 200 km in north–south extent, the lake level at the south shore should be 40 cm lower at periapsis than at apoapsis. Since Titan was within an Earth-day of periapsis during the T38 observation, the instantaneous tidal amplitude should have been near this maximum value.

If Unit 2 is an intertidal mudflat, then, the total elevation difference between its outer and inner margin must be ∼40 cm (or less for a non-rigid crust). On the T49 *Cassini* Titan encounter, the RADAR instrument will be able to acquire altimetry over Ontario Lacus' south shore that could test this prediction: if the altitude difference is large enough for the RADAR to measure (greater than 30 m), that would eliminate this formation mechanism from viability. Comparison to future VIMS observations of the margins of north polar lakes at varying latitudes and longitudes could provide further constraints on intertidal mudflats.

4.2. Unit 3

4.2.1. Frost

One idea for what might cause the near-IR-bright 'bathtub ring,' Unit 3, is methane/ethane frost. Such frost might reasonably be expected to be small-grained and bright and to exist in proximity to a source of humidity, as occurs with the lake-snow effect on Earth. However we do not favor this scenario for two reasons. First, the freezing point of methane and/or ethane, when mixed with atmospheric nitrogen, is depressed below the posited temperature at Titan's poles (Clark et al., in preparation). Secondly, the 'bathtub ring' borders the lake on all sides as seen by VIMS and ISS, instead of occurring just on one side, as might be expected if there were a favored wind direction.

4.2.2. Liquid-cleaned area

Titan's bright equatorial regions are thought to be covered with a thin veneer of organic or nitrile compounds derived from atmospheric photochemistry (Soderblom et al., 2007). Unit 3 might then be an area that is periodically inundated, removing its veneer. The spectrum of this unit shows both a relatively increased reflectivity within the lake in the 5-μm atmospheric window and a high 2.8/2.7 μm ratio. These characteristics are indicative of non-water-ice material, like that of the 5-μm bright regions Tui Regio and Hotei Regio (Barnes et al., 2005, 2006; McCord et al., 2008). That Unit 3 shows low water-ice content while channels and mountains cleared of veneer show enhanced water ice (Barnes et al., 2007b) argues against this hypothesis. However it could be that the crustal composition underlying Ontario Lacus is distinct from that underlying the equatorial bright unit, in which case the idea of veneer removal might still be possible.

4.2.3. Fine-grained condensate

Lakes on Earth that do not drain elsewhere build up concentrations of soluble compounds leached from minerals in the surrounding rocks. As the solvent evaporates away, the solute concentration increases until saturation, at which point it begins to precipitate. As a result, salt layers get deposited at the lakebottom. The extent of the salt layer is that of the lake's greatest extent, such that subsequent drawdown of liquid would leave a ring of salts surrounding the lake, hence the moniker 'bathtub ring' (see Fig. 7). On Titan, the solvent would be liquid methane and/or ethane. The 'salts' are harder to identify. The solubility of organic and nitrile species in methane- and ethane-rich solvents is low (10^{-7}–10^{-4}; Dubouloz et al., 1989) compared to that of polar salts in water on Earth. The solubility need not be as high as on Earth to produce detectable deposits, however, as VIMS sees only a few tens of microns into Titan's surface layer. If the resulting condensate lag deposits have sufficiently small grain sizes, then they might appear bright in near-infrared reflection as detected in Unit 3 by VIMS. In support of this hypothesis is a small outcrop of Unit 3 entirely surrounded by Unit 2 as seen in Fig. 4 near the

north end. This outcrop could be a small hill that was inundated at the lake's highstand but is exposed today.

5. Conclusion

The VIMS instrument on-board *Cassini* acquired four spectral mapping cubes of Titan's Ontario Lacus during the T38 encounter. These observations represent the finest spatial resolution view of Ontario Lacus to date. We use the four penecontemporaneous views of the same dark, uniform surface feature as a calibration target, which allows us to derive an analytical correction for atmospheric emission angle. A similar analysis allows a comparison of the atmospheric absorption within the 2.7 μm and 2.8 μm windows, implying that absorption at 2.7 μm is significantly greater than that at 2.8 μm.

When corrected for their emission angles and mosaiced, the VIMS cubes show a complex margin at the lake's southeastern shore. The center of the feature, revealed to be liquid by Brown et al. (2008), is bordered by two annuli. The inner annulus is ~10 km wide and shows an albedo that is low, but nonzero. This unit is only visible in the VIMS cubes with the lowest emission angles, and hence we do not know if it extends all of the way around the dark inner lake. Our preferred interpretation of this unit is that it represents lakebottom sediments exposed by either bulk changes in lake volume or tidal sloshing (in which case they could be called intertidal mudflats).

Exterior to the dark annulus is a bright margin. This margin extends all of the way around Ontario Lacus as shown by ISS context imagery, but with widely varying width of between a few hundred meters and 20 kilometers. The spectrum of the bright margin is consistent with a low water-ice content relative to the rest of Titan. We think that this unit may represent a deposit of fine-grained organic condensates from the lake that were laid down during a period of higher lake level in the past.

Based on these interpretations, the T38 VIMS observations imply prior lake-level changes in Ontario Lacus. The timescale, cause, and amplitude of the variations remain uncertain. Tidal sloshing occurs over weeks. Seasonal evaporation and precipitation should occur over 28 years. Longer-term changes in Titan's surface methane inventory and geologic processes occurring at Ontario Lacus specifically might take between 10^5 and 10^9 years (*e.g.* Sotin et al., 2005; Tobie et al., 2006). Future observations at differing orbital phase and season would allow us to constrain which processes are driving the lake-level changes and over what timescales. Knowledge of the amplitude of the changes will require reliable topographic information over Ontario Lacus with both high precision and fine spatial resolution — the T49 RADAR altimetry pass, should it occur, will shed light on these processes.

Acknowledgments

J.W.B. is supported by a NASA Postdoctoral Program Fellowship at NASA Ames Research Center administrated by Oak Ridge Associated Universities. J.W.B. also acknowledges support from the *Cassini* VIMS team. Thank you to the 2008 LPL beaches field trip participants for their comments and patience.

References

Barnes, J.W., Brown, R.H., Turtle, E.P., McEwen, A.S., Lorenz, R.D., Janssen, M., Schaller, E.L., Brown, M.E., Buratti, B.J., Sotin, C., Griffith, C., Clark, R., Perry, J., Fussner, S., Barbara, J., West, R., Elachi, C., Bouchez, A.H., Roe, H.G., Baines, K.H., Bellucci, G., Bibring, J.-P., Capaccioni, F., Cerroni, P., Combes, M., Coradini, A., Cruikshank, D.P., Drossart, P., Formisano, V., Jaumann, R., Langevin, Y., Matson, D.L., McCord, T.B., Nicholson, P.D., Sicardy, B., 2005. A 5-micron-bright spot on Titan: Evidence for surface diversity. Science 310, 92–95.

Barnes, J.W., Brown, R.H., Radebaugh, J., Buratti, B.J., Sotin, C., Le Mouelic, S., Rodriguez, S., Turtle, E.P., Perry, J., Clark, R., Baines, K.H., Nicholson, P.D., 2006. Cassini observations of flow-like features in western Tui Regio, Titan. Geophys. Res. Lett. 33, doi:10.1029/2006GL026843. 16204.

Barnes, J.W., Brown, R.H., Soderblom, L., Buratti, B.J., Sotin, C., Rodriguez, S., Le Mouèlic, S., Baines, K.H., Clark, R., Nicholson, P., 2007a. Global-scale surface spectral variations on Titan seen from Cassini/VIMS. Icarus 186, 242–258.

Barnes, J.W., Radebaugh, J., Brown, R.H., Wall, S., Soderblom, L., Lunine, J., Burr, D., Sotin, C., Le Mouélic, S., Rodriguez, S., Buratti, B.J., Clark, R., Baines, K.H., Jaumann, R., Nicholson, P.D., Kirk, R.L., Lopes, R., Lorenz, R.D., Mitchell, K., Wood, C.A., 2007b. Near-infrared spectral mapping of Titan's mountains and channels. J. Geophys. Res. (Planets) 112, doi:10.1029/2007JE002932. E11006.

Barnes, J.W., Brown, R.H., Soderblom, L., Sotin, C., Le Mouèlic, S., Rodriguez, S., Jaumann, R., Beyer, R.A., Buratti, B.J., Pitman, K., Baines, K.H., Clark, R., Nicholson, P., 2008. Spectroscopy, morphometry, and photoclinometry of Titan's dunefields from Cassini/VIMS. Icarus 195, 400–414.

Barnes, J.W., and 30 colleagues, 2009. VIMS spectral mapping observations of Titan during the Cassini prime mission. Planet. Space Sci., submitted for publication.

Brown, M.E., Bouchez, A.H., Griffith, C.A., 2002. Direct detection of variable tropospheric clouds near Titan's south pole. Nature 420, 795–797.

Brown, R.H., Baines, K.H., Bellucci, G., Bibring, J.-P., Buratti, B.J., Capaccioni, F., Cerroni, P., Clark, R.N., Coradini, A., Cruikshank, D.P., Drossart, P., Formisano, V., Jaumann, R., Langevin, Y., Matson, D.L., McCord, T.B., Mennella, V., Miller, E., Nelson, R.M., Nicholson, P.D., Sicardy, B., Sotin, C., 2004. The Cassini Visual and Infrared Mapping Spectrometer (VIMS) investigation. Space Sci. Rev. 15, 111–168.

Brown, R.H., Soderblom, L.A., Soderblom, J.M., Clark, R.N., Jaumann, R., Barnes, J.W., Sotin, C., Buratti, B., Baines, K.H., Nicholson, P.D., 2008. The identification of liquid ethane in Titan's Ontario Lacus. Nature 454, 607–610.

Dubouloz, N., Raulin, F., Lellouch, E., Gautier, D., 1989. Titan's hypothesized ocean properties—The influence of surface temperature and atmospheric composition uncertainties. Icarus 82, 81–96.

Fulchignoni, M., Ferri, F., Angrilli, F., Ball, A.J., Bar-Nun, A., Barucci, M.A., Bettanini, C., Bianchini, G., Borucki, W., Colombatti, G., Coradini, M., Coustenis, A., Debei, S., Falkner, P., Fanti, G., Flamini, E., Gaborit, V., Grard, R., Hamelin, M., Harri, A.M., Hathi, B., Jernej, I., Leese, M.R., Lehto, A., Lion Stoppato, P.F., López-Moreno, J.J., Mäkinen, T., McDonnell, J.A.M., McKay, C.P., Molina-Cuberos, G., Neubauer, F.M., Pirronello, V., Rodrigo, R., Saggin, B., Schwingenschuh, K., Seiff, A., Simões, F., Svedhem, H., Tokano, T., Towner, M.C., Trautner, R., Withers, P., Zarnecki, J.C., 2005. In situ measurements of the physical characteristics of Titan's environment. Nature 438, 785–791.

Griffith, C.A., Penteado, P., Rannou, P., Brown, R., Boudon, V., Baines, K.H., Clark, R., Drossart, P., Buratti, B., Nicholson, P., McKay, C.P., Coustenis, A., Negrao, A., Jaumann, R., 2006. Evidence for a polar ethane cloud on Titan. Science 313, 1620–1622.

Hayes, A., Aharonson, O., Callahan, P., Elachi, C., Gim, Y., Kirk, R., Lewis, K., Lopes, R., Lorenz, R., Lunine, J., Mitchell, K., Mitri, G., Stofan, E., Wall, S., 2008. Hydrocarbon lakes on Titan: Distribution and interaction with a porous regolith. Geophys. Res. Lett. 35, doi:10.1029/2008GL033409. 9204.

Jaumann, R., Brown, R.H., Stephan, K., Barnes, J.W., Soderblom, L.A., Sotin, C., Le Mouélic, S., Clark, R.N., Soderblom, J., Buratti, B.J., Wagner, R., McCord, T.B., Rodriguez, S., Baines, K.H., Cruikshank, D.P., Nicholson, P.D., Griffith, C.A., Langhans, M., Lorenz, R.D., 2008. Fluvial erosion and post-erosional processes on Titan. Icarus 197, 526–538.

Lorenz, R.D., 1994. Crater lakes on Titan: Rings, horseshoes and bullseyes. Planet. Space Sci. 42, 1–4.

Lorenz, R.D., Kraal, E.R., Eddlemon, E.E., Cheney, J., Greeley, R., 2005. Sea-surface wave growth under extraterrestrial atmospheres: Preliminary wind tunnel experiments with application to Mars and Titan. Icarus 175, 556–560.

Lorenz, R.D., Wall, S., Radebaugh, J., Boubin, G., Reffet, E., Janssen, M., Stofan, E., Lopes, R., Kirk, R., Elachi, C., Lunine, J., Mitchell, K., Paganelli, F., Soderblom, L., Wood, C., Wye, L., Zebker, H., Anderson, Y., Ostro, S., Allison, M., Boehmer, R., Callahan, P., Encrenaz, P., Ori, G.G., Francescetti, G., Gim, Y., Hamilton, G., Hensley, S., Johnson, W., Kelleher, K., Muhleman, D., Picardi, G., Posa, F., Roth, L., Seu, R., Shaffer, S., Stiles, B., Vetrella, S., Flamini, E., West, R., 2006. The sand seas of Titan: Cassini RADAR observations of longitudinal dunes. Science 312, 724–727.

Lunine, J.I., 1993. Does Titan have an ocean? A review of current understanding of Titan's surface. Rev. Geophys. 31, 133–149.

Lunine, J.I., Stevenson, D.J., Yung, Y.L., 1983. Ethane ocean on Titan. Science 222, 1229.

McCord, T.B., Hayne, P., Combe, J.-P., Hansen, G.B., Barnes, J.W., Rodriguez, S., Le Mouèlic, S., Baines, K.H., Brown, R.H., Buratti, B.J., Sotin, C., Nicholson, P., Jaumann, R., Nelson, R., Cassini VIMS team, 2008. Titan's surface: Search for spectral diversity and composition using the Cassini VIMS investigation. Icarus 194, 212–242.

Mitri, G., Showman, A.P., Lunine, J.I., Lorenz, R.D., 2007. Hydrocarbon lakes on Titan. Icarus 186, 385–394.

Porco, C.C., Baker, E., Barbara, J., Beurle, K., Brahic, A., Burns, J.A., Charnoz, S., Cooper, N., Dawson, D.D., Del Genio, A.D., Denk, T., Dones, L., Dyudina, U., Evans, M.W., Fussner, S., Giese, B., Grazier, K., Helfenstein, P., Ingersoll, A.P., Jacobson, R.A.,

Johnson, T.V., McEwen, A., Murray, C.D., Neukum, G., Owen, W.M., Perry, J., Roatsch, T., Spitale, J., Squyres, S., Thomas, P., Tiscareno, M., Turtle, E.P., Vasavada, A.R., Veverka, J., Wagner, R., West, R., 2005. Imaging of Titan from the Cassini spacecraft. Nature 434, 159–168.

Radebaugh, J., Lorenz, R.D., Lunine, J.I., Wall, S.D., Boubin, G., Reffet, E., Kirk, R.L., Lopes, R.M., Stofan, E.R., Soderblom, L., Allison, M., Janssen, M., Paillou, P., Callahan, P., Spencer, C., The Cassini Radar Team, 2008. Dunes on Titan observed by Cassini Radar. Icarus 194, 690–703.

Rannou, P., Montmessin, F., Hourdin, F., Lebonnois, S., 2006. The latitudinal distribution of clouds on Titan. Science 311, 201–205.

Rodriguez, S., Le Mouélic, S., Rannou, P., Tobie, G., Baines, K.H., Barnes, J.W., Griffith, C.A., Hirtzig, M., Pitman, K.M., Sotin, C., Brown, R.H., Buratti, B.J., Clark, R.N., Nicholson, P.D., 2009. Cloud activity on Titan: Seasonal changes and tidal effects. Nature, submitted for publication.

Roe, H.G., de Pater, I., Macintosh, B.A., McKay, C.P., 2002. Titan's clouds from Gemini and Keck Adaptive Optics imaging. Astrophys. J. 581, 1399–1406.

Roe, H.G., Bouchez, A.H., Trujillo, C.A., Schaller, E.L., Brown, M.E., 2005. Discovery of temperate latitude clouds on Titan. Astrophys. J. 618, L49–L52.

Sagan, C., Dermott, S.F., 1982. The tide in the seas of Titan. Nature 300, 731–733.

Soderblom, L., Kirk, R.L., Lunine, J.I., Anderson, J.A., Baines, K.H., Barnes, J.W., Barrett, J.M., Brown, R.H., Buratti, B.J., Clark, R.N., Cruikshank, D.P., Elachi, C., Janssen, M.A., Jaumann, R., Karkoschka, E., Le Mouèlic, S., Lopes, R.M., Lorenz, R.D., McCord, T.B., Nicholson, P.D., Radebaugh, J., Rizk, B., Sotin, C., Stofan, E.R., Sulcharski, T.L., Tomasko, M.G., Wall, S.D., 2007. Correlations between Cassini VIMS spectra and RADAR SAR images: Implications for Titan's surface composition and the character of the Huygens Probe Landing Site. Planet. Space Sci. 55, 2025–2036.

Sotin, C., Jaumann, R., Buratti, B.J., Brown, R.H., Clark, R.N., Soderblom, L.A., Baines, K.H., Bellucci, G., Bibring, J.-P., Capaccioni, F., Cerroni, P., Combes, M., Coradini, A., Cruikshank, D.P., Drossart, P., Formisano, V., Langevin, Y., Matson, D.L., McCord, T.B., Nelson, R.M., Nicholson, P.D., Sicardy, B., Le Mouèlic, S., Rodriguez, S., Stephan, K., Scholz, C.K., 2005. Release of volatiles from a possible cryovolcano from near-infrared imaging of Titan. Nature 435, 786–789.

Stiles, B.W., and 13 colleagues, Cassini RADAR Team, 2008. Determining Titan's spin state from Cassini RADAR images. Astron. J. 135 (5), 1669–1680.

Stofan, E.R., Elachi, C., Lunine, J.I., Lorenz, R.D., Stiles, B., Mitchell, K.L., Ostro, S., Soderblom, L., Wood, C., Zebker, H., Wall, S., Janssen, M., Kirk, R., Lopes, R., Paganelli, F., Radebaugh, J., Wye, L., Anderson, Y., Allison, M., Boehmer, R., Callahan, P., Encrenaz, P., Flamini, E., Francescetti, G., Gim, Y., Hamilton, G., Hensley, S., Johnson, W.T.K., Kelleher, K., Muhleman, D., Paillou, P., Picardi, G., Posa, F., Roth, L., Seu, R., Shaffer, S., Vetrella, S., West, R., 2007. The lakes of Titan. Nature 445, 61–64.

Tobie, G., Lunine, J.I., Sotin, C., 2006. Episodic outgassing as the origin of atmospheric methane on Titan. Nature 440, 61–64.

Turtle, E.P., Perry, J.E., McEwen, A.S., DelGenio, A.D., Barbara, J., West, R.A., Dawson, D.D., Porco, C.C., 2009. Cassini imaging of Titan's high-latitude lakes, clouds, and south-polar surface changes. Geophys. Res. Lett., doi:10.1029/2008GL036186, in press.

West, R.A., Brown, M.E., Salinas, S.V., Bouchez, A.H., Roe, H.G., 2005. No oceans on Titan from the absence of a near-infrared specular reflection. Nature 436, 670–672.